

Unified Measure of Goodness and Optimal Design of Spectral Sensitivity Functions

Shuxue Quan,[▲] Noboru Ohta,[▲] Roy S. Berns,[▲] and Xiaoyun Jiang

Munsell Color Science Laboratory, Center for Imaging Science, Rochester Institute of Technology, Rochester, New York

Naoya Katoh[▲]

PNC Development Center, Sony Corporation, Tokyo, Japan

To evaluate and optimally design spectral sensitivity functions for color input devices, a metric that incorporates practical, significant requirements is desired. The candidate metrics are Vora–Trussell’s μ -factor, a metric based on geometrical difference, and the proposed Unified Measure of Goodness, or UMG, which simultaneously considers the imaging noise and its propagation, colorimetric reproduction accuracy and multi-illuminant color correction. A systematic approach is presented to searching for an optimal set of spectral sensitivity functions from among the complete combinations of the given filter components. Comparative computation results show that μ -factor is not a competent metric for the optimal design of camera spectral sensitivity functions while UMG is able to pick out the optimum successfully. Furthermore, the ultimate optimal set has been obtained by selecting the set with highest μ -factor value from the sub-optimal collection obtained with UMG. This hierarchical approach comprehensively considers the advantages of both quality metrics. The candidates of the optimal sets based on the given filter components are experimentally tested and presented in the end of the article.

Journal of Imaging Science and Technology 46: 485–497 (2002)

Introduction

The design and image quality of any color imaging device depend on the human visual system and real world constraints. The human visual color perception can be described by the tristimulus theory that involves the linear combination of three different photoreceptor types with known spectral sensitivities in the visible range. The Commission Internationale de l’Eclairage (CIE) has characterized the normal human visual color perception with color-matching functions for a standard observer and defined standard color spaces, including the non-uniform CIE XYZ and uniform CIELAB spaces.¹ These standards are fundamental for colorimetry and for the transformation and sharing of color information. Color input devices such as cameras and scanners that seek for colorimetric reproduction (as well as color appearance match or preferred color reproduction) of object colors must take into account the characteristics of the human visual system in their design and in the understanding of the output data from the physical sensors. Although these input devices have reached

reasonable performance today, their color reproduction is still perceptibly different from the original scene. Major reasons for this are the difficulties of selection and fabrication of transmittance filter sets that are suitable for color imaging devices. Basically two primary factors—the non-Luther condition due to the practical limitations in the designing and manufacturing of these filters and the intrinsic imaging noise in the capture process, limit their color reproduction accuracy. The optimal design of the spectral sensitivity functions should account for both factors. A criterion for evaluating and optimally designing the spectral sensitivities is therefore desirable.

The concept of the so-called “quality factor” was first introduced by Neugebauer.² For various purposes, quite a few quality metrics^{2–8} have been introduced so far. All these metrics for evaluating and designing spectral sensitivities striving for colorimetric reproduction can be categorized into two types. The first type describes the geometrical difference between the subspaces of color matching functions and spectral sensitivity functions. These quality factors are often sample-independent and do not consider the imaging noise, but only consider the difference between the subspaces through linear transformation. Typical metrics are Neugebauer’s q -factor,² for the evaluation of single imaging channel, Vora–Trussell’s q -factor extension, or μ -factor,³ for the colorimetric evaluation of multi-channel system with an arbitrary number of channels, and the Color Quality Factor (CQF),⁵ already used in the industry for the colorimetric evaluation of individual imaging channels. The second type describes the

Original manuscript received February 4, 2002

▲ IS&T Member

©2002, IS&T—The Society for Imaging Science and Technology

minimized average color error between the estimated and reference color attributes for a set of user defined samples of reflectance spectra in CIE color spaces. The linear transformation from camera RGB signals to CIE XYZ values is determined by minimizing the color error and a data dependent metric can be defined based upon this procedure. Imaging noise may or may not be considered during the minimization procedure. In this category, there are Shimano's Q_{st} and Q_{sf} metrics,^{7,8} minimizing the average color error in CIE XYZ space without noise consideration, Tajima's indices,⁴ taking account of object color spectral characteristics of principle components, Hung's CRI (Color Rendering Index),⁵ and Sharma-Trussell's Figure of Merit (FOM),⁵ an extensive but pretty complicated quality factor, minimizing the color error in a perceptually uniform color space while taking account of the white noise in the recording process. A few above-mentioned simpler quality factors can be attributed to the special forms of FOM.⁶ We extend the FOM as Unified Measure of Goodness (UMG) in this study so that it includes both the signal independent and signal dependent imaging noises, e.g., dark noise and shot noise, as well as multi-illuminant color correction, to be described in the following section. Notice that the data dependent metrics may show different trends for different data sets, selection of standard set for those metrics should be cautious and consistent. The 24 Macbeth ColorChecker patches are used as standard samples in our computation due to the widespread use of this target in color imaging area and its representativeness of a much larger set, such as the Vrhel-Trussell dataset containing 354 color samples.^{9,10}

A lot of effort has been put into the filter design issue. Ohta started the evaluation and optimization of sensitivities in subtractive imaging systems.^{11,12} Wolski, and co-workers reviewed the major work done before them,¹³ including Davies and Wyszecski,¹⁴ Engelhardt and Seitz,¹⁵ Vrhel and Trussell,¹⁶ Vora and Trussell.^{3,17} Tsumura, and co-workers optimized three channel Gaussian-shaped filters with noise presence by minimizing CIE color difference with simulated annealing.¹⁵ Wolski and co-workers also optimized the sensor response functions for colorimetry of reflectance and emissive objects under multiple illuminants,¹³ and the optimization is carried out in CIELAB color space with smoothness constraint. Sharma and Trussell also carried out the optimal searching of transmittance filters,¹⁹ but not with their proposed FOM metric, they were looking for the nonnegative filters with the presence of white noise in the similar way as Vrhel and Trussell did.¹⁶ Notice that all of those efforts were successful in some aspects, but also have some respective disadvantage. A satisfactory solution should take into account, both data independent and data dependent performance, as well as signal independent and signal dependent noises, and the objective function of optimization should be implemented within a perceptually uniform color space or color appearance space. Furthermore, most of these studies give optimal curves in theoretical sense, which need be approximated with manufacturer's filter component set during fabrication process. This approximation will induce error resulting in the fabricated curves deviated from the ideally optimal ones, which may make the theoretically optimal set practically not optimal any more. The optimal design approach would optimize the imaging channels directly as a parameterized model of the filter manufacturing process, e.g., the selection of the filter

components with their thickness used in each channel. In such a case, it is unnecessary to assume the spectral sensitivities to be smooth, since in practice most of them are not strictly smooth, also the designed spectral sensitivities are guaranteed to be non-negative, because the filter components used are always non-negative. We will demonstrate this new strategy to optimize filters for a high-end digital camera in this article.

The article is organized as follows. A data independent metric, μ -factor will be briefly introduced, followed by a detailed description of the proposed data dependent metric, *unified measure of goodness*. Both metrics are chosen as criteria to the optimal design of spectral sensitivities for colorimetric reproduction. Hierarchical approaches are adapted, and results of optimal design from two approaches are reported and compared.

The Colorimetric Quality Factors

Vora and Trussell's μ -Factor

The Luther condition requires that the spectral sensitivities be the linear combinations of the color matching functions.²⁰ This strict relationship may not easily follow in the real world, although intuitively the closer the approximation of the Luther condition is, the better colorimetric reproduction performance is expected. μ -Factor introduced by Vora and Trussell characterizes the deviation of the Luther condition, which has been widely discussed.^{3-5,21} In brief μ -factor describes the geometrical difference between the fundamental subspaces²² of the CIE color matching functions (CMF) A and some set of camera spectral sensitivities (SS) S :

$$\mu_A(S) = \frac{\text{Trace}\{O^T U U^T O\}}{\text{Trace}\{U U^T\}} \quad (1)$$

where O and U are the corresponding fundamental subspaces of A and S , and $\text{Trace}\{\cdot\}$ calculates the summation of diagonal elements in a matrix. Similar equation without using the orthonormal space concept can also be used to characterize this difference.²¹ Equation (1) is an elegant description of the requirement of S , but it is incomplete to deal with the practical problems, e.g., the imaging noise. It is possible to design and fabricate a set with high colorimetric spectral sensitivity functions in terms of μ -factor but, at the same time, with poor practical colorimetric reproduction performance, because some spectral sensitivity functions may amplify much more noise than others in the signal processing chain (Fig. 1). On the other side, the human visual system may prefer less noise appearance to colorimetric accuracy. Therefore this factor only described one aspect of requirements for spectral sensitivities.

CCD Noise Model

Electronic imaging is a process of converting photons to electrons. Noise is intrinsic in electronic imaging process, and is found commonly existed in the following forms: photon noise or shot noise, dark current noise, fixed pattern noise, photo response non-uniformity noise, reset noise, $1/f$ noise and quantization noise.^{23,24} It is application dependent to select which types of noise should be considered. In this application, noises are categorized into two types: signal independent noise, represented by Gaussian-type noise, such as dark noise and thermal noise, and signal dependent noise, represented by shot noise, or photon noise. It is known

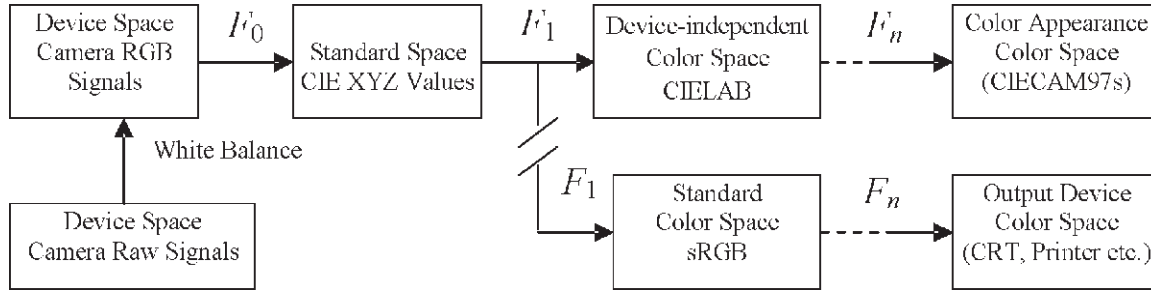


Figure 1. Signal processing pipeline in a digital camera, where F s are functions describing signal transformations.

that the photon arrival behavior fulfills Poisson distribution, so the signal uncertainty, or noise variance equals the noise mean.

In this study, the following noise model was used:^{9,24,25}

$$E(\text{noise} : \eta) = 0 \quad (2)$$

$$\text{var}(\text{noise} : \eta) = \sigma_\eta^2 = \sigma_d^2 + \rho^2 \mu_i = \sigma_d^2 + \rho^2 \sigma_i^2 \quad (3)$$

where σ_d^2 denotes the dark noise variance, μ_i represents the input signal intensity, σ_i^2 denotes the shot noise variance, and ρ describes the total photon-electron conversion quantum efficiency coefficient of CCD. Equation (3) was experimentally verified for typical digital camera by Burns.²⁵ Because Eq. (3) applies to the number of photons in practical device characterization, for convenience, the noise levels are represented with digital counts relative to the digital count of maximal signal. The dark noise is the variation of signal digital counts while the camera shutter is turned off, and the real coefficient associated with shot noise ($k = \rho^2$) can be obtained by fitting Eq. (3) with a series of signal levels and the corresponding signal variations.

Figure 1 illustrates the raw device signals are white balanced, converted to CIE XYZ values, and transformed into target color space to match output devices in the signal processing chain. The noise in the capture stage will be propagated and amplified by the series of linear and nonlinear transformations. Root-mean-square (RMS) noise can be defined in the target space as the noise level for a given set of spectral sensitivities and illuminant.

Unified Measure of Goodness

Since noise is unavoidable, and practically is not limited to signal independent noise as assumed in FOM, a metric representing color reproduction performance should include both signal independent noise and signal dependent noise. This new metric is proposed by taking account of the following properties: the average color difference for an ensemble of standard reflectance samples in a perceptually uniform color space is minimized; the input noise, which is modeled as mixture of shot noise and dark noise, is propagated into the target color space while the signal is processed, and a linear matrix converting camera RGB to CIE XYZ is obtained through the minimization of noise propagation. Furthermore, a strategy striving for multi-illuminant color correction is incorporated. All these important aspects are *unified* into a single metric—UMG.

Let r denote reflectance of object color, L_o denote the diagonal matrix with the spectral power distribution of viewing illuminant along its diagonal, L_c denote the

taking illuminant also in diagonal form. The average color difference as Euclidean distance in the uniform color space is minimized using the following *mean squared color error* as cost function:

$$\varepsilon = E\left\{\|F(t) - F(F_0 t_c)\|^2\right\} \quad (4)$$

where $t = A^T L_o r = A^T L_r$ is the reference CIE XYZ values, $t_c = S^T L_c r + \eta = G^T r + \eta$ is the camera output signal with noise modeled by Eqs. 2-3, $A_L = L_c A$, $G = L_c S$, F_0 linearly transforms t_c into CIE XYZ to match t , $t' = F_0 t_c$, and

$$F(\bullet) = F_n(\dots F_2(F_1(\bullet))) \quad (5)$$

sequentially transforms the tristimulus values into the interested high-level target color space, e.g., CIELAB, or CIECAM97s via linear or nonlinear transformations F_1, \dots, F_n as shown in Fig. 1. For deriving our metric, F_0 is assumed to be a linear matrix, although in reality, a number of techniques may be implemented to define this transformation, including polynomial transformation, look-up table etc. If F_1, \dots, F_n are approximately differentiable with continuous first partial derivatives, a first-order Taylor expansion provides a fairly accurate locally linear approximation for each of them:

$$F_i(x + \Delta x) - F_i(x) = J_{F_i}(x) \Delta x \quad (6)$$

where J_{F_i} is the Jacobian matrix consisting of first-order partial derivatives. With the law of chains for first derivatives,

$$F(x + \Delta x) - F(x) = \prod_{i=1}^n J_{F_i}(F_{i-1}(\dots F_1(x))) \Delta x = J_F(x) \Delta x \quad (7)$$

where J_F is the combined Jacobian matrix. By applying Eqs. (6) and (7), Eq. (4) can be approximated by

$$\begin{aligned} \varepsilon \cong \varepsilon_l &= E\left\{\|J_F(t)(t - F_0 t_c)\|^2\right\} \\ &= E\left\{\|J_F(t)t - J_F(t)F_0 t_c\|^2\right\} \end{aligned} \quad (8)$$

To minimize Eq. (8) and obtain a close-form of F_0 , we start from the simple least-squares technique. For a least-squares problem of finding optimal b such that $Yb = x$, or

$$\min\left\{\varepsilon = \|x - Yb\|^2\right\} \quad (9)$$

where ε is regression error, measurement x is fitted with Y by b . The solution of b is obtained with Moore–Penrose (MP) pseudo-inverse²²

$$b = (Y^T Y)^{-1} Y^T x \quad (10)$$

Therefore the minimized mean square error is

$$\begin{aligned} \varepsilon_{\min} &= \|x - Yb\|^2 = \|x - Y(Y^T Y)^{-1} Y^T x\|^2 \\ &= (x - Y(Y^T Y)^{-1} Y^T x)^T (x - Y(Y^T Y)^{-1} Y^T x) \quad (11) \\ &= x^T x - x^T Y(Y^T Y)^{-1} Y^T x = \alpha(x) - \tau(x, Y) \end{aligned}$$

where $\alpha(x) \equiv x^T x$ and $\tau(x, Y) \equiv x^T Y(Y^T Y)^{-1} Y^T x$. The ratio

$$q = \frac{\tau(x, Y)}{\alpha(x)} = 1 - \frac{\varepsilon_{\min}}{\alpha(x)} \quad (12)$$

defines the goodness of fitting. If $q \rightarrow 1$, $\varepsilon_{\min} \rightarrow 0$, the fitting becomes perfect.

Equation (8) is not in the apparent form of Eq. (9). The *Kronecker* product and *vec* operator²⁶ can be applied to convert it to Eq. (9), as did by Sharma and Trussell,^{5,27} and Wolski and co-workers.¹³ The *Kronecker* product transforms two matrices $A = (a_{ij})$ and $B = (b_{st})$ into a matrix $C = A \otimes B = (a_{ij} b_{st})$, and the *vec* operator transforms a matrix into a vector by stacking its columns one underneath the other. For arbitrary matrices, T , U , V , and W with appropriate sizes, the following results hold:^{26,27}

$$\begin{aligned} (T + U) \otimes (V + W) &= T \otimes V + T \otimes W + U \otimes V + U \otimes W \\ (T \otimes U)(V \otimes W) &= TV \otimes UW \\ (T \otimes U)^T &= T^T \otimes U^T \\ \text{vec}(UVW) &= (W^T \otimes U) \text{vec}(V) \\ (T \otimes U)(V \otimes W) &= TV \otimes UW \quad (13) \\ (T \otimes U)^{-1} &= T^{-1} \otimes U^{-1} \\ \text{trace}(TUVW) &= (\text{vec} W^T)^T (V^T \otimes T) \text{vec} U \end{aligned}$$

Applying Eq. (13) onto Eq. (8),

$$\begin{aligned} J_F(t) A_L^T r &= \text{vec}(J_F(t) A_L^T r) = (r^T \otimes J_F(t)) \text{vec}(A_L^T) \\ J_F(t) F_0 [G^T r + \eta] &= \text{vec}(J_F(t) F_0 [G^T r + \eta]) = [(G^T r + \eta)^T \otimes J_F(t)] \text{vec}(F_0) \quad (14) \end{aligned}$$

For notational simplicity, denote

$$\begin{aligned} b &= \text{vec}(F_0), \\ x &= (r^T \otimes J_F(t)) \text{vec}(A_L^T), \\ Y &= (G^T r + \eta)^T \otimes J_F(t). \end{aligned}$$

Then

$$\begin{aligned} \varepsilon_l(A_L, G, F_0) &= E\{\|x - Yb\|^2\} \\ &= E\{\|x\|^2\} - 2E\{x^T Y\}b + b^T E\{Y^T Y\}b \quad (15) \end{aligned}$$

Notice that Eq. (15) has similar form to Eq. (9), clearly a minimum exists and the optimal transformation b_{opt} :

$$\text{vec}(F_{0opt}) = b_{opt} = \left[E\{Y^T Y\} \right]^{-1} E\{Y^T x\} \quad (16)$$

Now applying Eq. (16) onto Eq. (15), the corresponding minimal error is similar to Eq. (11):

$$\begin{aligned} \varepsilon_l(A_L, G, F_{0opt}) &= E\{\|x\|^2\} - 2E\{x^T Y\}b_{opt} + b_{opt}^T E\{Y^T Y\}b_{opt} \\ &= E\{\|x\|^2\} - E\{x^T Y\} \left[E\{Y^T Y\} \right]^{-1} E\{Y^T x\} \quad (17) \end{aligned}$$

where

$$\begin{aligned} &E\{Y^T Y\} \\ &= E\left\{ \left[(G^T r + \eta) \otimes J_F^T(t) \right] \left[(G^T r + \eta)^T \otimes J_F(t) \right] \right\} \\ &= E\left\{ (G^T r + \eta) (G^T r + \eta)^T \otimes J_F^T(t) J_F(t) \right\} \\ &= E\left\{ G^T r r^T G + G^T r \eta^T + \eta^T G \eta \right\} \otimes J_F^T(t) J_F(t) \\ &= E\left\{ G^T r r^T G \otimes J_F^T(t) J_F(t) \right\} + \dots \quad (18) \\ &= (G^T \otimes I_3) E\{r r^T \otimes J_F^T(t) J_F(t)\} (G \otimes I_3) \\ &\quad + (G^T \otimes I_3) E\{r \eta^T \otimes J_F^T(t) J_F(t)\} \\ &\quad + E\{\eta^T \otimes J_F^T(t) J_F(t)\} (G \otimes I_3) + E\{\eta \eta^T \otimes J_F^T(t) J_F(t)\} \end{aligned}$$

where I_3 denotes the 3×3 identity matrix. Also,

$$\begin{aligned} &E\{Y^T x\} \\ &= E\left\{ \left[(G^T r + \eta) \otimes J_F^T(t) \right] \left[r^T \otimes J_F(t) \right] \text{vec}(A_L^T) \right\} \\ &= E\left\{ \left[G^T r r^T + \eta^T \right] \otimes J_F^T(t) J_F(t) \right\} \text{vec}(A_L^T) \quad (19) \\ &= (G^T \otimes I_3) E\{r r^T \otimes J_F^T(t) J_F(t) + \eta^T \otimes J_F^T(t) J_F(t)\} \text{vec}(A_L^T), \end{aligned}$$

$$\begin{aligned} E\{\|x\|^2\} &= E\left\{ \text{vec}(A_L^T)^T (r \otimes J_F^T(t)) (r^T \otimes J_F(t)) \text{vec}(A_L^T) \right\} \\ &= \text{vec}(A_L^T)^T E\{r r^T \otimes (J_F^T(t) J_F(t))\} \text{vec}(A_L^T). \quad (20) \end{aligned}$$

According to the aforementioned CCD imager noise model, the recording noise η is zero mean and dependent of signal, or the object reflectance spectrum r . The noise variance is

$$E\{\eta \eta^T\} = \sigma_\eta^2 = \sigma_d^2 + k\mu_i = \sigma_d^2 + kG^T r \quad (21)$$

where r is the object sample reflectance, G denotes the product of spectral sensitivities S and illuminant spectral

power distribution L_c , and k is the constant describing the shot noise property according to signal level μ_i . The noise mean is

$$E[\eta] = 0. \quad (22)$$

For specific r_i , the noise can be treated as independent variable from signal since the noise variance in Eq. (21) is constant, thus:

$$\begin{aligned} & E\{\eta r^T \otimes J_F^T(t) J_F(t)\} \\ &= \frac{1}{n_{sample}} \sum_{i=1}^{n_{sample}} E\{\eta_i\} E\{r_i^T\} \otimes E\{J_F^T(t_i) J_F(t_i)\} \quad (23) \\ &= 0 \end{aligned}$$

$$E\{r \eta^T \otimes J_F^T(t) J_F(t)\} = \left[E\{\eta r^T \otimes J_F^T(t) J_F(t)\} \right]^T = 0 \quad (24)$$

$$\begin{aligned} & E\{\eta \eta^T \otimes J_F^T(t) J_F(t)\} \\ &= \frac{1}{n_{sample}} \sum_{i=1}^{n_{sample}} E\{n_i \eta_i^T\} \otimes E\{J_F^T(t_i) J_F(t_i)\} \\ &= \frac{1}{n_{sample}} \sum_{i=1}^{n_{sample}} \text{diag}(\sigma_d^2 + k G^T r_i) \otimes [J_F^T(t_i) J_F(t_i)] \\ &= \frac{1}{n_{sample}} \sum_{i=1}^{n_{sample}} \text{diag}(\sigma_d^2) \otimes [J_F^T(t_i) J_F(t_i)] \quad (25) \\ &+ k \frac{1}{n_{sample}} \sum_{i=1}^{n_{sample}} \text{diag}(G^T r_i) \otimes [J_F^T(t_i) J_F(t_i)] \\ &= K_{\sigma_d} \otimes E\{J_F^T(t) J_F(t)\} + k E\{\text{diag}(G^T r) \otimes [J_F^T(t) J_F(t)]\} \end{aligned}$$

where K_{σ_d} is the dark noise covariance matrix, $\text{diag}(\cdot)$ and convert a vector to a diagonal matrix, n_{sample} is the total number of samples in the standard testing target, and $t_i = A^T r_i$ is the tristimulus values of the i^{th} sample.

The optimal transformation from camera RGB to CIE XYZ is given by

$$\begin{aligned} \text{vec}(F_{0opt}(A_L, G)) &= \arg \min_{F_0} \varepsilon_l(A_L, G, F_0) = b_{opt} \\ &= \left[(G^T \otimes I_3) S_r (G \otimes I_3) + S_\eta \right]^{-1} (G^T \otimes I_3) S_r \text{vec}(A_L^T) \quad (26) \end{aligned}$$

where

$$S_r = E\left\{ (r r^T) \otimes (J_F^T(t) J_F(t)) \right\} \quad (27)$$

$$\begin{aligned} S_\eta &= E\left\{ \eta \eta^T \otimes J_F^T(t) J_F(t) \right\} \\ &= K_{\sigma_d} \otimes E\left\{ J_F^T(t) J_F(t) \right\} \quad (28) \\ &+ k E\left\{ \text{diag}(G^T r_i) \otimes [J_F^T(t_i) J_F(t_i)] \right\} \end{aligned}$$

The minimal color error in Eq. (8) can then be written as

$$\varepsilon_{\min} = \alpha(A_L) - \tau(A_L, G) \quad (29)$$

where

$$\alpha(A_L) = \text{vec}(A_L^T)^T S_r \text{vec}(A_L^T) \quad (30)$$

$$\begin{aligned} \tau(A_L, G) &= \text{vec}(A_L^T)^T S_r (G \otimes I_3) \\ &\times \left[(G^T \otimes I_3) S_r (G \otimes I_3) + S_\eta \right]^{-1} (G^T \otimes I_3) S_r \text{vec}(A_L^T) \quad (31) \end{aligned}$$

In Eq. (29), $\alpha(A_L)$ may be interpreted as the total colorimetric information of object colors, and $\tau(A_L, G)$ is the colorimetric information that can be obtained with the spectral sensitivity functions in G . A new metric for single viewing-taking illuminant pair can be defined as Eq. (32). Note that the mean square color error is minimized, to obtain a linear relationship between UMG and averaged color error, Eq. (32) is further linearized into Eq. (33):⁵

$$q(A_L, G, F) = \frac{\tau(A_L, G)}{\alpha(A_L)} \quad (32)$$

$$\theta = 1 - \sqrt{1 - q(A_L, G, F)} \quad (33)$$

Since the taking (recording) and viewing illuminant may be different, a quality factor can be defined for each pair of taking and viewing illuminants if multiple interested illuminants need be considered. For example, if the viewing illuminant can be chosen from a set of illuminants $\{L_{v_1}, L_{v_2}, \dots, L_{v_n}\}$ and the taking illuminant can be chosen from another set of illuminants $\{L_{c_1}, L_{c_2}, \dots, L_{c_m}\}$ a quality factor matrix \mathbf{M} can be defined as follows:

$$\mathbf{M} = \begin{bmatrix} \theta_{11} & \theta_{12} & \theta_{13} & \cdots & \theta_{1m} \\ \theta_{21} & \theta_{22} & \theta_{23} & \cdots & \vdots \\ \theta_{11} & \theta_{11} & \theta_{11} & \cdots & \vdots \\ \vdots & \vdots & \vdots & \ddots & \vdots \\ \theta_{n1} & \theta_{n2} & \theta_{n3} & \cdots & \theta_{nm} \end{bmatrix} \quad (34)$$

where θ_{ij} is the metric described by Eq. (33) corresponding to illuminant pair (L_{v_i}, L_{c_j}) .

Therefore, a comprehensive quality factor UMG for all the taking-viewing-illuminant pairs may be defined as the weighted average of all elements in \mathbf{M} :

$$\Theta = \frac{1}{nm} \sum_{i=1}^n \sum_{j=1}^m w_{ij} \theta_{ij} \quad \text{while} \quad \sum_{i=1}^n \sum_{j=1}^m w_{ij} = 1 \quad (35)$$

where w_{ij} is the weight determined by camera manufacturers, quantifying the importance of the corresponding illuminant pair (L_{v_i}, L_{c_j}) .

The typical relationship between the UMG defined in CIELAB and the average color difference for a set of reflectance samples in CIELAB has been shown as roughly linear for UMG value in reasonable range. In Fig. 2, the dark noise RMS was assumed to be 20 electrons, the photon-electron conversion quantum

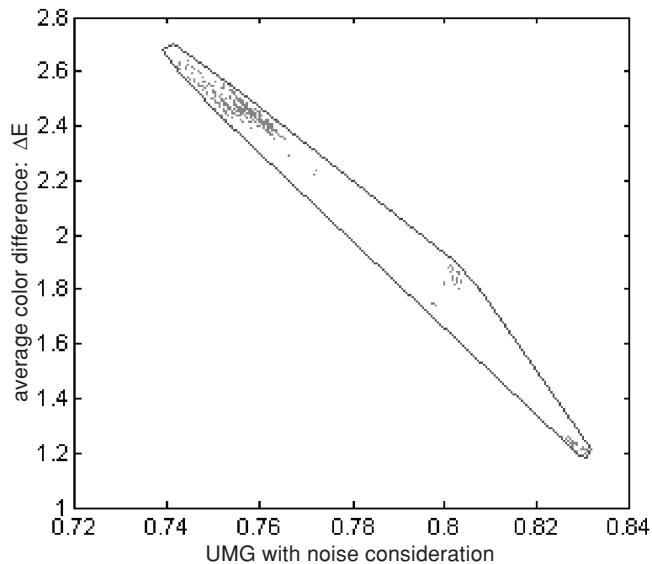


Figure 2. The relationship between UMG with noise consideration and average color difference ΔE^* .

efficiency is assumed to be 80%, and the maximal signal level corresponds to 10^4 electrons, 500 sets of spectral sensitivities generated from the application described below were used as test targets, the UMG value and RMS noise in CIELAB was calculated for each set of SS and represented as a dot in the plot. It also shows that the set of SS with larger UMG value roughly corresponds to a smaller RMS noise.

Notice that UMG requires much more computation than μ -factor, due to the fact that evaluating UMG needs calculating multiple statistical information for all object samples in the standard set, it is recommended to avoid large-scale UMG computation. The significant difference between UMG and FOM is that a practically verified CCD imaging noise model is incorporated with UMG. Since the shot noise dominates when signal is at or above average level, the signal independent noise assumption is incorrect, reflected into filter design, the filters obtained with UMG should offer more confidence than those obtained with FOM. The detailed performance comparison between FOM and UMG is not the focus of this article but will be discussed in the future.

Application: Designing Color Filters for Colorimetric Reproductions

Background

A high-end black and white digital camera system, Roper Scientific Photometrics Quantix™, was purchased at the Munsell Color Science Laboratory. It is essentially a panchromatic black and white camera since no color filters were designed for it yet. In this practical application, multiple channel spectral sensitivity functions will be determined from a set of available bandpass filters, infrared cutoff filters and longpass glass filters. The known data are the total spectral sensitivity of the electronic sensor, including the optimal lens and the total infrared cutoff filter, and the transmittance spectra of given basic filter components. Optimally, three to five spectral sensitivity functions for colorimetric reproduction with noise consideration are expected.

The normalized total monochrome detector spectral sensitivity function is measured on the spot, which

includes the spectral sensitivity of CCD sensor, the transmittance of the optical lenses and a total IR cutoff filter, as shown in Fig. 3(a). This black and white sensitivity is measured for a given setup of the camera, and the sensor sensitivity is assumed constant once the camera configuration is fixed.

There are 14 bandpass glass filters (VG-type and BG-type Schott Glass) available. The transmittance of filter with 3 mm thickness is shown in Fig. 3(b). These filters are important to shape the green and blue channels for digital cameras when they are combined with longpass filters. It is possible to obtain the red channel as well if they are combined with some infrared cutoff filters.

There are 7 basic infrared cutoff glass filters (2 BG-type, 5 KG-type Schott Glass) in the set, whose transmittance is shown in Fig. 3(c) when the thickness is 3 mm. The two BG-type filters have rich variation from 400 nm to 650 nm, while the five KG-type filters varies from 600 nm to 700 nm, but changes slowly between 400 nm and 600 nm, which is a crucial wavelength interval for color image capturing.

The transmittance of the 19 basic longpass cutoff glass filters (GG-type, OG-type and RG-type Schott Glass) is shown in Fig. 3(d), where the thickness is still 3 mm. Their transmittance spectra typically have sharp edges and do not vary too much if the filter thickness changes within certain range, such as 1 mm – 3 mm.

The transmittance of all these filters is based on a thickness of 3 mm, which can be easily varied to 2 mm and 1 mm according to the manufacturer. For 2 mm and 1 mm thickness, according to Bouger's Law,²⁸ the corresponding transmittance can be approximately represented as:

$$T_{2\text{ mm}} = T_{3\text{ mm}}^{2/3}, T_{1\text{ mm}} = T_{3\text{ mm}}^{1/3} \quad (36)$$

If a filter composed to isolate a certain channel is obtained by superimposing several filter elements with different thickness and the reflection between two layers is omitted, its total transmittance can be written as:

$$T_{\text{Total}} = \prod_{i=1}^k T_i^{x_i/3} \quad (37)$$

where x_i and T_i are the thickness and transmittance of the corresponding filter element i . The total channel spectral sensitivity including CCD spectral sensitivity function SS_{CCD} is

$$SS = SS_{\text{CCD}} \cdot T_{\text{Total}}. \quad (38)$$

To achieve the transmittance of blue and green channel sensitivities, let the bandpass filters have thickness choices of 3 mm, 2 mm and 1 mm, optionally combined with longpass filters. The BG-type of IR cutoff filters are more important than the KG filters, and the thickness of each basic IR can be chosen from 3 mm, 2 mm and 1 mm, totally 21 IR filters. The longpass filters have sharp cutoff property, their thickness variation does not change their transmittance shape very much, so only thickness of 3 mm (or 2 mm/1 mm) may be selected in order to reduce computation amount, otherwise a total of 57 longpass filters are available for three thickness choices. To obtain the transmittance of red spectral sensitivity function, the combination of longpass filters and IR cutoff filters, or the combination of bandpass filters and IR cutoff filters may be used. If

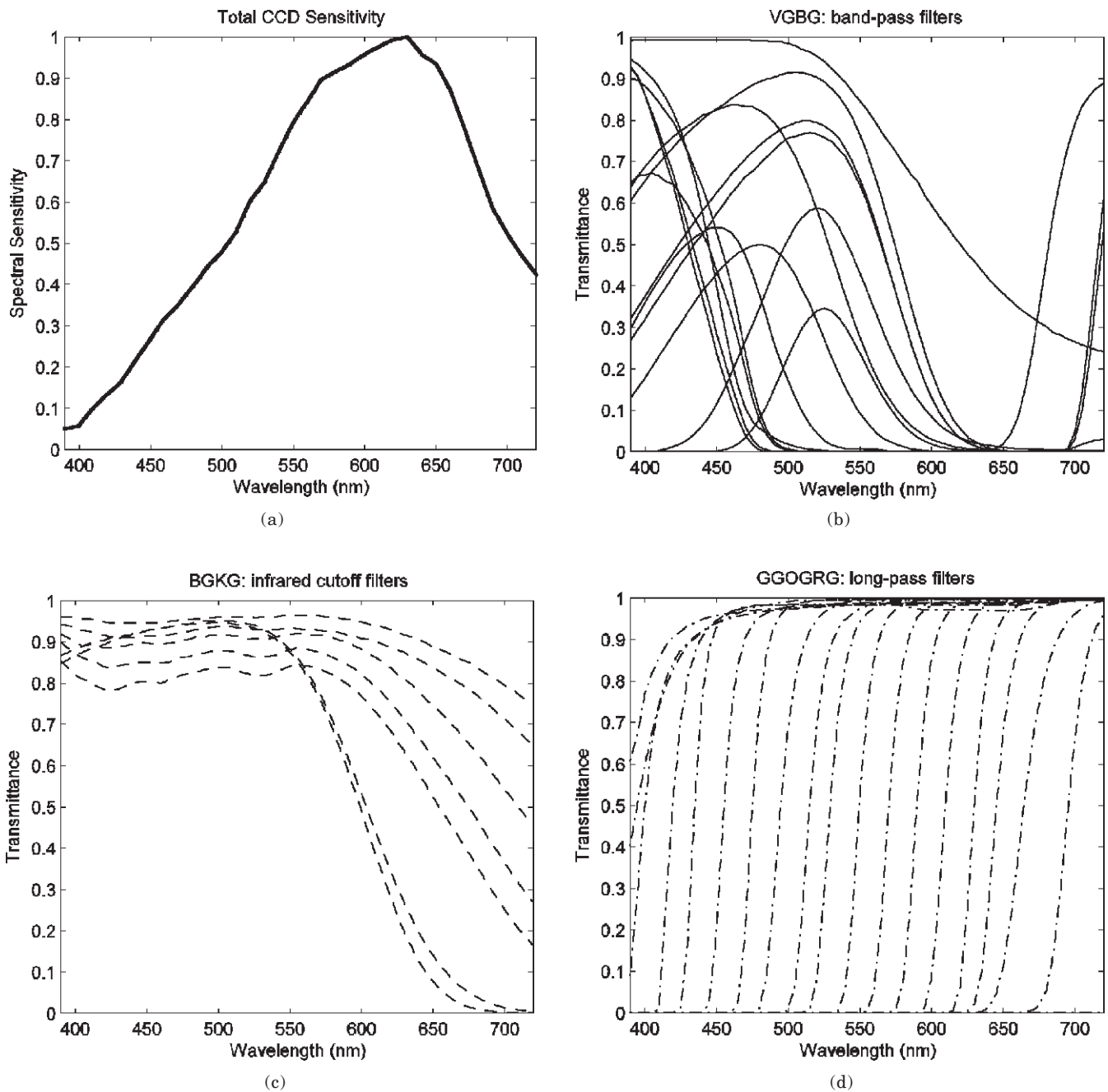


Figure 3. (a) The measured total spectral sensitivity function for CCD, optical lens and infrared cutoff filter as a whole; (b) Transmittance spectra of bandpass filter components; (c) Transmittance spectra of infrared cutoff filter components; (d) Transmittance spectra of longpass filter components.

the number of filter components for each channel is limited to two, all possible filter combinations can be formed as follows:

- Bandpass: $14 \times 3 = 42$ (may be independently used)
- IR cutoff: $7 \times 3 = 21$ (not used independently)
- Longpass: $19 \times 3 = 57$ (may be independently used)
- Bandpass \times IR cutoff: $42 \times 21 = 882$
- Bandpass \times Long-pass: $42 \times 57 = 2934$
- Longpass \times IR: $57 \times 21 = 1197$

The total number of all filters is 4572.

To find the optimal K filters from among these filters, the total combination is 4572^K , for example, the

computation iterations would be 9.56×10^{10} for $K = 3$. It can be seen that even for searching three optimal filters from the set, the computation of single metric evaluation will take too much time. Some analysis on the filter property has to be carried out beforehand in order to reject the apparent non-optimal combinations and reduce the computation load significantly.

Pre-selection of Spectral Sensitivity Functions

It is a huge computational load to obtain an optimal set with a brute force search. We need to pre-select filters in the first step to reduce computation. Our early research¹ on general optimization of hypothetical spectral sensitivity functions shows that, filters with a sin-

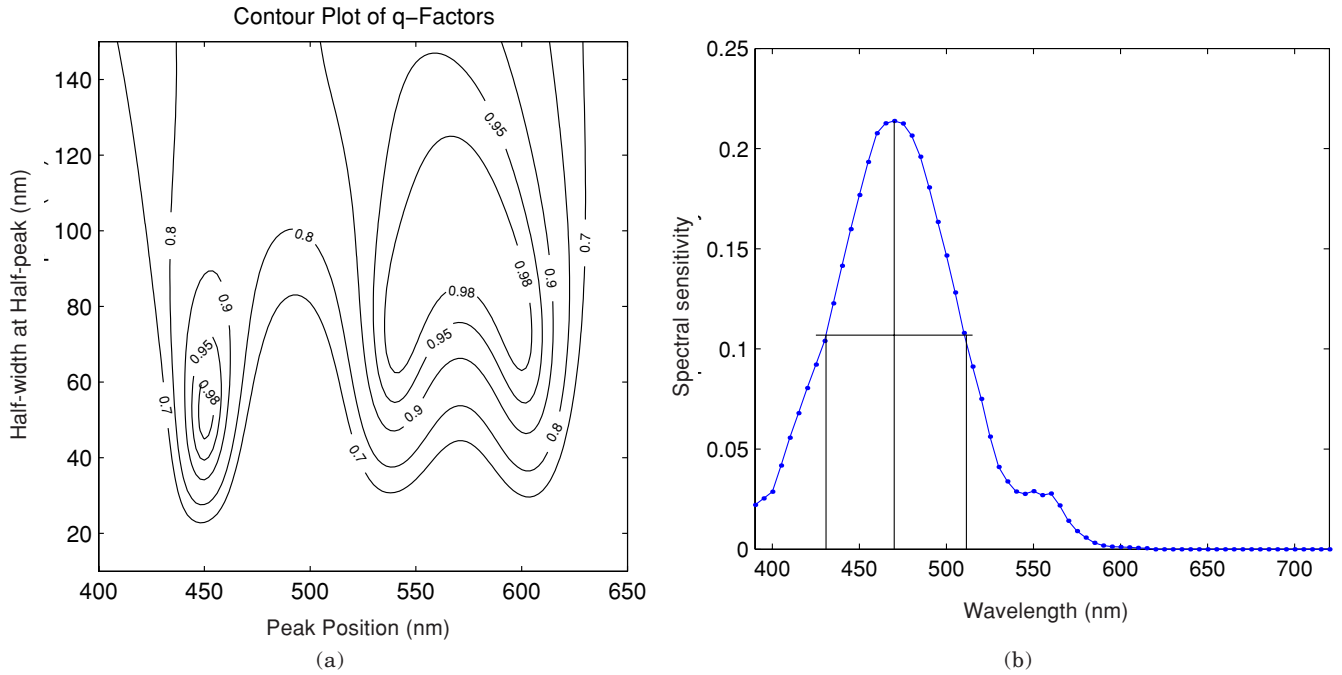


Figure 4. (a) Preferred peak positions and half-widths obtained with q -factor by setting various confidence levels; (b) Estimation of the width at half-maximum for any spectral sensitivity functions with a single primary peak.

gle primary peak are preferred, and the possible peak position of blue channel is located between 400 nm and 500 nm (strictly 420 – 470 nm), that of green channel between 500 nm and 600 nm (strictly 520 – 560 nm), and that of red channel between 550 nm and 650 nm (strictly 570 – 620 nm), obtained with q -factor evaluation and shown in Fig. 4(a). The blue channel choices then become 517, for green channel, 1869, and for red channel, 1368, if the extended peak position ranges are applied. This will lead to the reduction of the amount of computation to $517 \times 1869 \times 1368 = 1.3219 \times 10^9$, about two percent computation amount of the raw brute force search. If the strict peak position ranges of the three channels are used, the three numbers are further reduced to 391, 1075 and 1049. The corresponding computation load (4.409×10^8) is even less since the search range is even smaller. It is possible that some optimal combinations may be discarded when peak position pre-selection is applied.

For better performance under noisy environment, the widths of sensitivity functions cannot be too wide, or too narrow. Figure 4(a) also shows the optimal sensitivity functions should limit their peak width at half maximum to less than 120 nm. By assuming the area of the enclosed rectangle is half of the area under the single peaked sensitivity curve, as illustrated in Fig. 4(b), the full-width, at peak-to-peak, can easily be estimated. Those filters with width less than 120 nm and strict peak position ranges are then obtained. The possible choices for blue, green and red channels are now reduced to 384, 601 and 402. This reduces the total evaluation iterations to 9.2×10^7 , which is a more suitable computation to be finished within days using current typical desktop personal computers.

Optimization with μ -factor

The evaluation of spectral sensitivities with μ -factor is much faster but it does not consider noise, while the evaluation with UMG is slow, but it considers more

practical issues of spectral sensitivities. It is a better choice if advantages of both metrics can be utilized in designing optimal spectral sensitivities. A few tests were conducted for two different approaches, that is, optimization with μ -factor then refined with UMG, or optimization with UMG then refined with μ -factor. In the first trial, 400 optimal combinations will be obtained with μ -factor since the evaluation of μ -factor is much faster.

Since the measured noise model of the specific camera was not available, the noise is determined by Signal-to-Noise Ratio (SNR), which implies signal independent, zero-mean white noise. The SNR is defined as

$$\begin{aligned}
 SNR(dB) &= 10 \log_{10} \left(\frac{\text{trace}(G^T r r^T G)}{n_{\text{sample}} J \sigma_{\eta}^2} \right) \\
 &= 10 \log_{10} \left(\frac{\text{trace}(G^T K_r G)}{J \sigma_{\eta}^2} \right) \quad (39)
 \end{aligned}$$

where J is the number of channels, K_r is the correlation matrix of the standard samples. Therefore the noise variance (per channel) is specified as

$$\sigma_{\eta}^2 = \frac{1}{J} \frac{\text{trace}(G^T K_r G)}{10^{SNR(dB)/10}} \quad (40)$$

Strictly the signal dependent noise was not currently considered according to Eqs. (39) and (40). In fact, for the same CCD, lens and IR cutoff filter, different color filters should give different SNR performance, so the assumption of the same SNR for all color filter sets is not strictly correct. The corresponding UMG values are calculated for the 400 sets by assuming the system SNR to be 45 dB, which is more or less a reasonable performance level for most color imaging devices, or 80 dB, that is, the noise is near zero. The most favorable set of

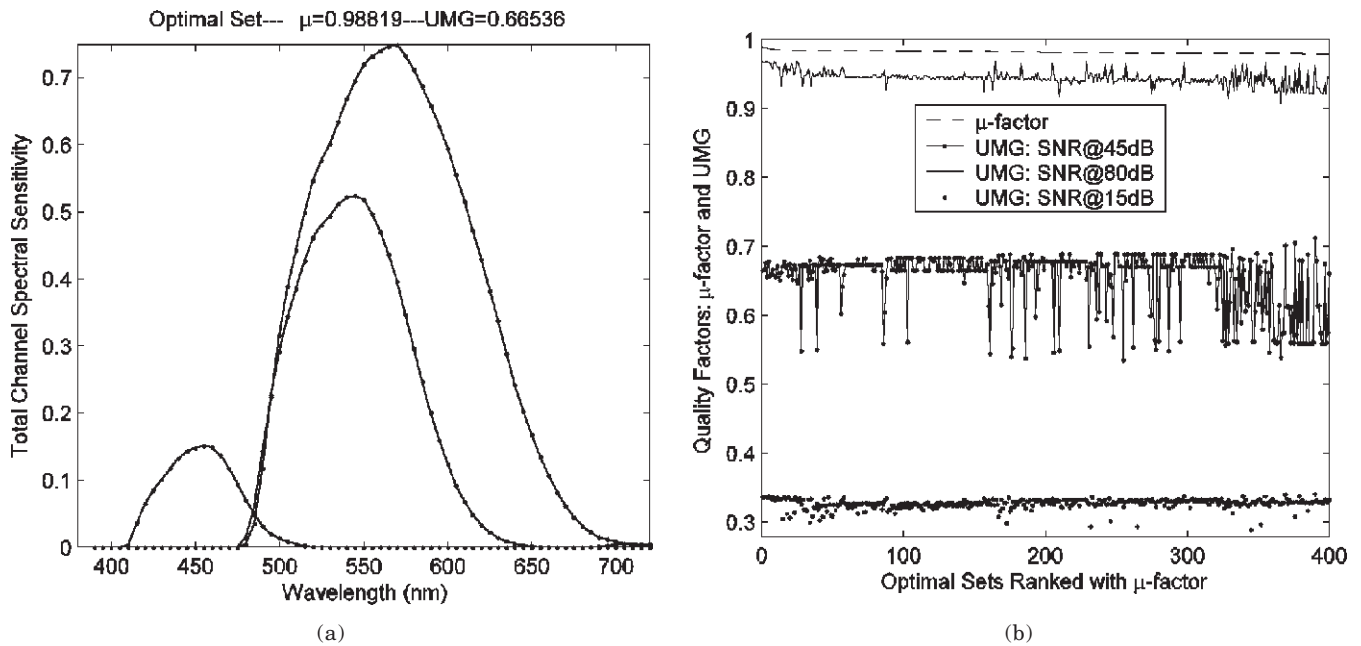


Figure 5. (a) The “optimal” sensitivity function set obtained with μ -factor; the shape is not desired; (b) the UMG at various SNR levels and μ -factor values of the 400 sets of spectral sensitivities with highest μ -factor.

three filters in terms of μ -factor is shown in Fig. 5(a), with a μ -factor of 0.988. But this kind of shapes as a whole is weird and is not desired when compared with available camera spectral sensitivities sets,⁶ since the transmittance of the green channel is totally enveloped under the red channel. Examining all 400 sets, most of them have such kind of unfavorable shapes. They have high μ -factor (>0.98), but their UMG values at 45 dB SNR are too small (<0.70), as shown in Fig. 5(b). When the noise is free from the system (SNR = 80 dB), it's not surprising that the set of sensitivity functions with high μ -factor corresponds to high UMG values, although their shapes are not ideally the same as the set in Fig. 5(a). It seems that the desired truly optimal filter sets with smaller μ -factor values but much larger UMG values are pushed back by those “pseudo” optimal sets.

In order to dig out the optimal set, the searching range can be reduced by using only one width for the longpass filters, i.e., 2 mm, because width does not affect their cutoff properties very much. The choices for red, green and blue channels are then reduced to 114, 206 and 150. The first 400 optimal sets in terms of μ -factor are obtained and the UMG values for these sets at 45 dB SNR are calculated. Figure 6(a) demonstrates the different trends of μ -factor and UMG values. The μ -factor values are very close for all of these sets (>0.965), but obviously, some sets have much higher UMG values than the others. The set of filters with highest UMG value among the 400 sets are shown in Fig. 6(b). Its UMG is 0.807 (45 dB) and μ -factor is 0.966. Quite a few similar sets have close UMG and μ -factor values. Their shapes are very similar to this optimal candidate and can be treated as alternative optima. Most of the other sets with higher μ -factor values but lower UMG values do not have such kind of favorable shape, their shapes are rather more like Fig. 5(a), which are not preferred. Therefore sensitivity sets like Fig. 6(b) are better choices than those from the first trial.

From above it can be seen that when the typical noise (SNR is about 45 dB) is superimposed onto the signal as in the real world, the optimal sets obtained through

noise analysis can perform better than the sets not from noise consideration. Furthermore, when the noise becomes too great, for example, the signal-to-noise ratio is reduced to about 15 dB in dark illumination, they do not show overwhelming noise proofing any more, since the noise has overshadowed the input signal. If the SNR goes very high (~ 80 dB), the noise can be omitted; filter sets with high μ -factor values usually perform well in terms of color difference.

Optimization with UMG

Our third trial is to optimize the spectral sensitivity functions by directly evaluating UMG for the reduced combinations after peak-width pre-selection process. Because UMG depends on the data set, illuminants, and noise level, these parameters are kept the same as the previous experiments. As expected, it is much more time-consuming to go through all combinations. A mainstream desktop computer required about twenty times of time more than it required finishing the evaluation with μ -factor. Figure 7 shows the optimal set obtained from this approach, which is selected with μ -factor from among the 500 sets of optimum candidates obtained with UMG. This optimal set has a μ -factor value of 0.935, smaller than the optimal set shown in Fig. 6, but its UMG performance is much better, 0.933. The difference between the two sets is that, the sensitivities in Fig. 7 have closer peak sensitivities for three channels than that in Fig. 6. It would be interesting to know, which would perform better in practical imaging experiment. Their difference may be further determined with additional properties, subjective evaluation, or chosen by experienced manufacturers.

Experimental Results and Discussion

The optimal filter set obtained in the second trial was fabricated by Schott, the glass filter provider, and the total spectral sensitivities for all three channels were measured and compared with the designed curves, as

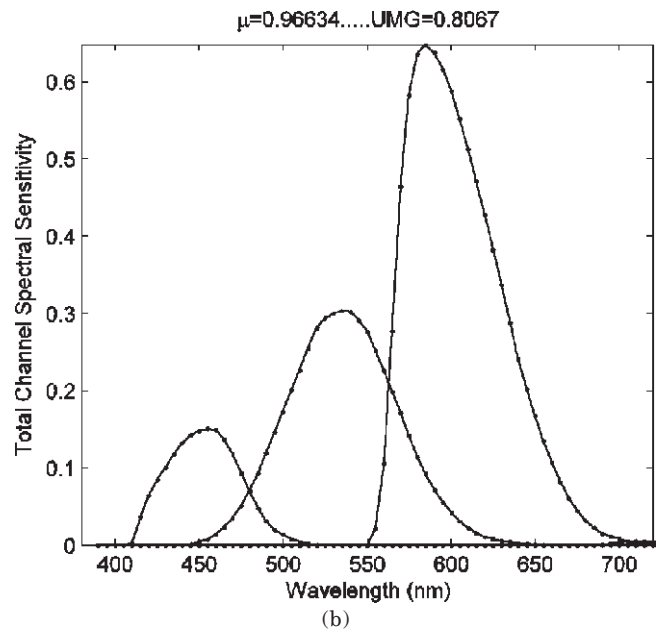
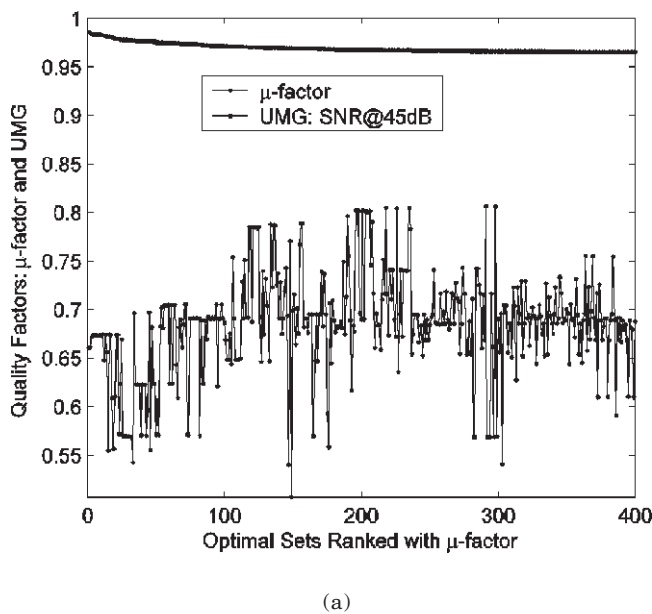


Figure 6. (a) UMG and μ -factor values of the 400 sets obtained with μ -factor, only a thickness of 2 mm is used for longpass filters; (b) The optimal set with highest UMG values among the 400 sets obtained with μ -factor.

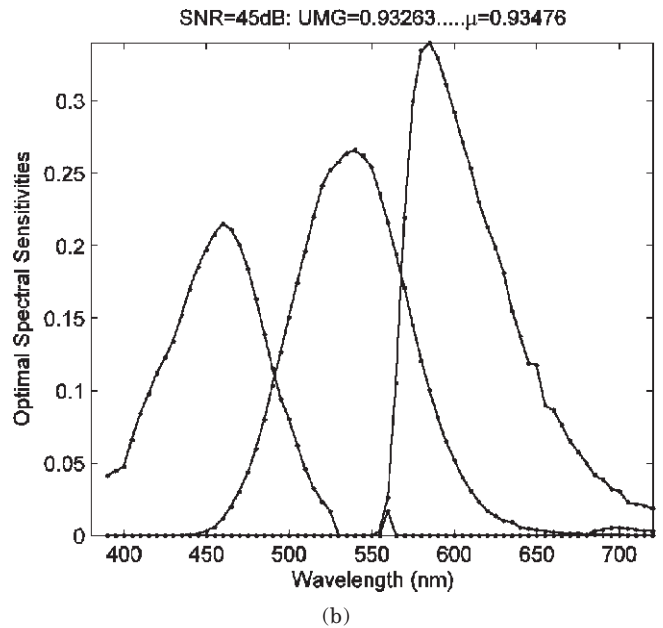
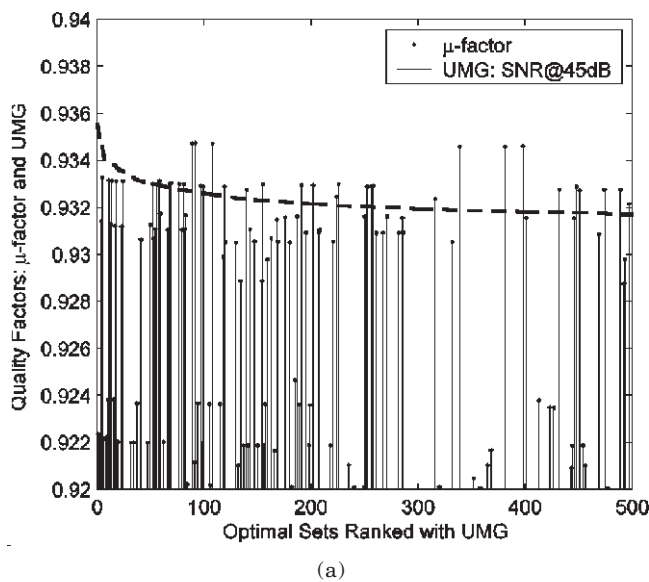


Figure 7. (a) μ -Factor and UMG values of the 500 optimal filter sets obtained with UMG; (b) The optimal set with maximum UMG value.

shown in Fig. 8(a). The designed and measured curves overlap very well with each other, except the red channel has a scale factor, perhaps the thickness of glass components were not well controlled. A simulated experiment of imaging Macbeth ColorChecker patches was carried out in order to compare the performance of four sets of spectral sensitivities: designed set 1 from the second trial 2, fabricated set 1, designed set 2 from the third trial, and the measured IBM Pro/3000 spectral sensitivity functions as shown in Fig. 8(b). Since different cameras have different noise performance, for comparison, the SNR is assumed at 45 dB for all sets. The simulated results were listed in Table I. For

comparison, the multiple quality factor values were also listed in the table. Table I verified that the performance of the designed and fabricated set 1 is very close. The designed set 2 is similar to the IBM camera, but the latter has a high sensitivity in the blue channel which makes it a better choice when tungsten light is used. In experimental testing, a Macbeth ColorChecker was captured with the fabricated color filters; the predicted and calculated average and maximal color difference performance are listed in Table II. The experimental color differences are only slightly worse than the predicted, which means the designed color filters are highly colorimetric spectral sensitivities.

TABLE I. Quality Factors and Simulated Color Differences for the Four Sets of Spectral Sensitivities. Four Pairs of Taking and Viewing Illuminants Were Used (D65, A, F2 and Scanlite). Scanlite Has a SPD Similar to CIE A, is the Practical Light Source Used with the Photometrics Quantix Camera

Taking – Viewing Illuminants →		(D65 – D65)	(A – A)	(F2 – F2)	(S – S)
Sensitivities	μ -Factor	UMG	UMG	UMG	UMG
Designed Set 1	0.967	0.861	0.653	0.780	0.668
Fabricated Set 1	0.956	0.891	0.745	0.859	0.759
Designed Set 2	0.937	0.935	0.858	0.910	0.866
IBM Pro/3000	0.932	0.934	0.912	0.928	0.916

Color Difference Performance for Macbeth ColorChecker Patches					
Designed Set 1	Mean ΔE_{94}^*	0.80	1.82	0.87	1.65
	Max ΔE_{94}^*	2.40	3.13	2.63	2.98
Fabricated Set 1	Mean ΔE_{94}^*	1.24	1.23	1.12	1.23
	Max ΔE_{94}^*	4.02	4.23	3.88	4.20
Designed Set 2	Mean ΔE_{94}^*	0.70	0.92	0.62	0.91
	Max ΔE_{94}^*	1.72	2.13	1.52	2.13
IBM Pro/3000	Mean ΔE_{94}^*	0.65	0.52	0.66	0.53
	Max ΔE_{94}^*	1.53	1.36	1.53	1.34

TABLE II. Experimental Color Difference Performance with Macbeth ColorChecker as Imaging Target

	Mean ΔE_{94}^*	Mean ΔE_{ab}^*	Max ΔE_{94}^*	Max ΔE_{ab}^*
Predicted RGB SS	0.98	1.79	3.63	6.02
Experimental RGB SS	1.13	2.13	3.08	5.39

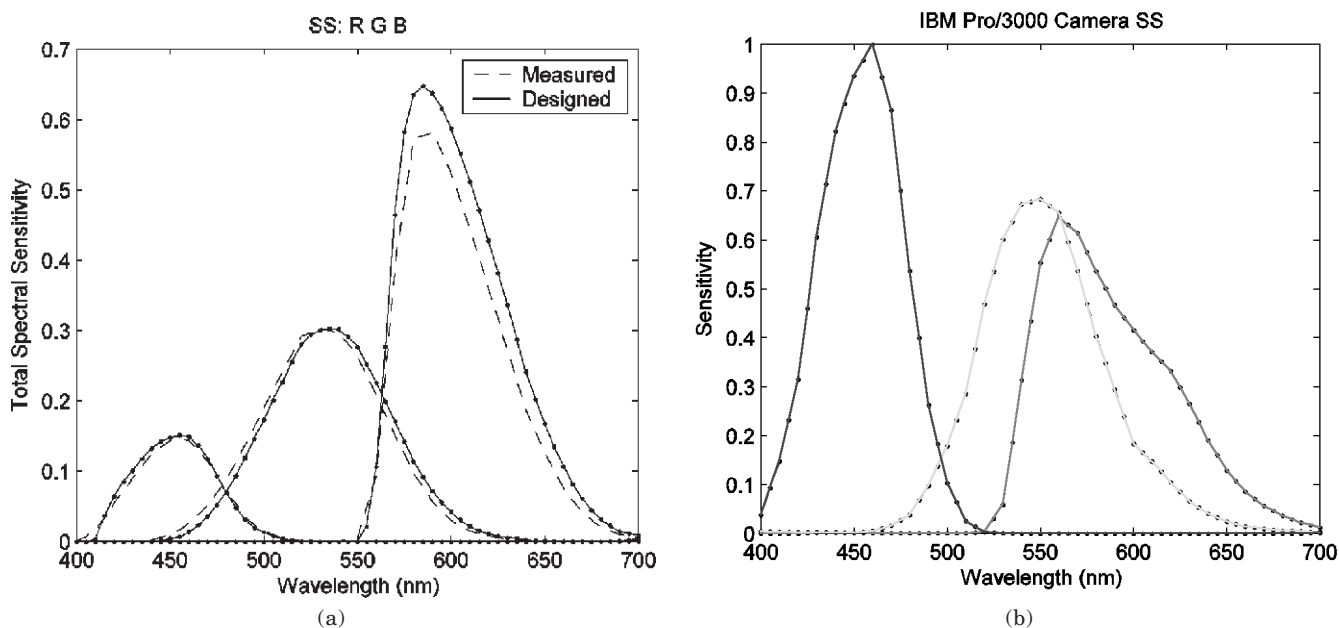


Figure 8. (a) The designed and fabricated spectral sensitivity set 1; (b) The measured IBM Pro/3000 camera spectral sensitivity functions.

In another aspect, the predicted and captured camera output digital counts should have good consistency, which is expected to be a linear relationship between them. A real experiment was conducted to take images on Kodak Gray Scale patches. Figure 9 shows the predicted and measured digital counts of all three channels have very high linearity. The color difference of transforming RGB signals to CIE XYZ is 0.03 (average) and 0.108 (maximum) for converting the predicted digital counts to CIE XYZ, and 1.01 (average) and 4.22

(maximum) for converting experimental camera output digital counts to CIE XYZ. It is reasonable that the experimental test yielded a larger color difference because of more system uncertainties involved in practice, such as the measurement of CCD sensitivity difference between the fabricated and designed filters, and other unexpected noise sources.

The ultimate selection of optimal spectral sensitivities may rely on some additional properties. Different weights may be assigned to different metrics (e.g., μ -

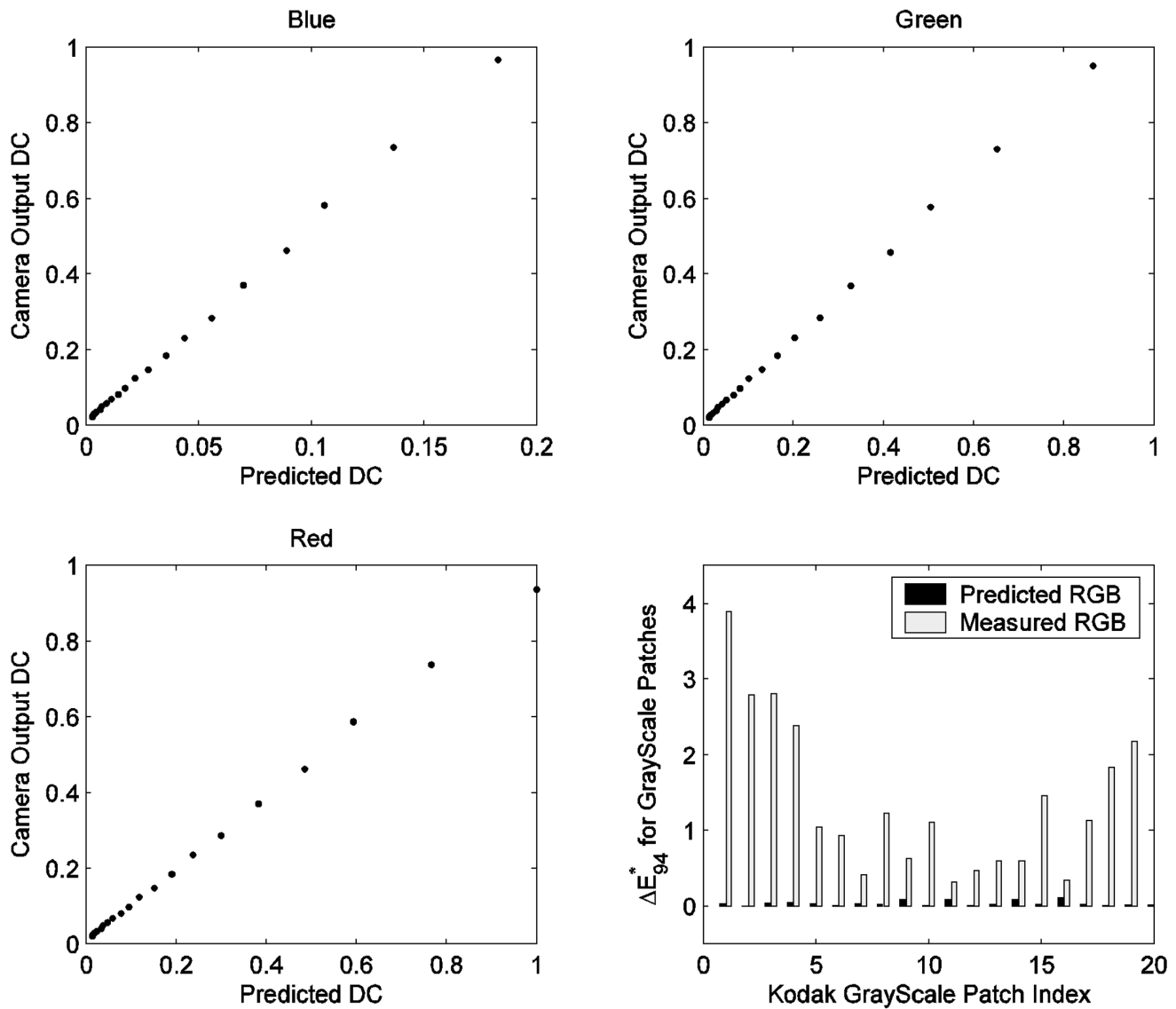


Figure 9. The linearity relationship between the predicted and recorded camera output digital counts (DC) for each channel, and color difference performance of imaging Kodak GrayScale.

factor and UMG at different noise levels) to form a comprehensive quality metric. In addition, the optimization of four or five spectral sensitivities can be carried out based on the optimization results of three channels. This study has shown that the optimal three channels can achieve very good colorimetric performance. Adding one or two channels can obtain more information on object colors, and usually a larger quality factor value is expected. The peak positions of the additional spectral sensitivity functions should locate differently from the peak positions of the primary ones in order to reduce noise amplification and maximize acquisition information for multi-spectral imaging of object reflectance. This will be further explored and presented in the future.

Conclusions

An optimal set of filters should satisfy two primary requirements: first, the subspace of the camera spectral sensitivity functions should approximate that of color

matching functions as much as possible; and second, the estimation of object colors from noise contaminated camera signals should approximate the measurement of these object colors in a uniform color space. Basically, μ -factor indicates whether a sensitivity set is colorimetric or not in a noiseless condition. But in the real world, noise may discard some colorimetric sets obtained with a metric without considering noise. By taking into account more practical factors such as noise, UMG is able to pick out genuine colorimetric sensitivity functions. It was shown in the study that a set of sensitivity functions with a relatively poor μ -factor may have a reasonably good UMG, and reproduce object colors nicely. Furthermore, a set of sensitivity functions with the highest μ -factor may correspond to very low UMG value, or a large average color difference, which means that it is not a good choice to be implemented in practice. Future work will incorporate a measured noise model into the optimal selection of color filters and compare the optimal results from both UMG and FOM. \blacktriangle

Acknowledgment. The current research is supported by SONY Corp. The authors thank Dr. Francisco Imai and Mr. Mitchell R. Rosen for useful discussions or comments on the research and the article.

References

1. S. Quan, N. Ohta, M. Rosen, and N. Katoh, Fabrication tolerance and optimal design of spectral sensitivities for color imaging devices, *Proc. IS&T PICS 2001 Conference*, IS&T, Springfield, VA, 2001, pp. 277-282.
2. H. E. J. Neugebauer, Quality factor for filters whose spectral transmittances are different from color mixture curves, *J. Opt. Soc. Amer.* **46**(10), 821-824 (1956).
3. P. L. Vora and H. J. Trussell, Measure of goodness of a set of color-scanning filters, *J. Opt. Soc. Amer. A*, **10**(7), 1499-1508 (1993).
4. J. Tajima, New quality measures for a set of color sensors, *Proc. Fourth IS&T/SID Color Imaging Conference: Color Science, Systems, and Applications*, IS&T, Springfield, VA, 1996, pp. 25-28.
5. G. Sharma and H. J. Trussell, Figure of merit for color scanners, *IEEE Trans. Image Processing* **6**, 990 (1997).
6. P. C. Hung, Comparison of camera quality indexes, *Proc. IS&T Color Imaging Conference 2000*, IS&T, Springfield, VA, 2000, pp. 167-171.
7. N. Shimano, Colorimetric evaluation of color image acquisition systems I, *J. Photo. Elec.* **29**(5), 506-516 (2000).
8. N. Shimano, Colorimetric evaluation of color image acquisition systems II, *J. Photo. Elec.* **29**(5), 517-520 (2000).
9. S. Quan, *Evaluation and Optimal Design of Spectral Sensitivities for Digital Color Imaging*, Ph.D. Dissertation, Rochester Institute of Technology, Rochester, NY, USA (2002).
10. M. J. Vrhel and H. J. Trussell, Color correction using principal components, *Color Res. Appl.* **17**, 328 (1992).
11. N. Ohta, Evaluation of Spectral Sensitivities, *Photo. Sci. Eng.* **25**(3), 101-107 (1981).
12. N. Ohta, Optimization of Spectral Sensitivities, *Photo. Sci. Eng.* **27**(5), 193-201 (1983).
13. M. Wolski, C. A. Bouman and J. P. Allebach, Optimization of sensor response functions for colorimetry of reflective and emissive objects, *IEEE Trans. Image Processing*, **5**, 507-517 (1996).
14. W. E. R. Davies and G. Wyszecki, Physical approximation of color mixture functions, *J. Opt. Soc. Amer.* **52**, 679-685, (1962).
15. K. Engelhardt and P. Seitz, Optimum color filters for CCD digital cameras, *Appl. Opt.* **32**(16), 3015-3023 (1993).
16. M. J. Vrhel and H. J. Trussell, Filter Considerations in color correction, *IEEE Trans. Image Processing* **3**, 147 (1994).
17. P. L. Vora and H. J. Trussell, A mathematical method for designing a set of color scanning filters, *Proc. SPIE* **1912**, 322-329 (1993).
18. N. Tsumura and co-workers, Optimal Spectral Transmittance of color filters, *Proc. IS&T's 50th Annual Conference*, IS&T, Springfield, VA, 1998, 373-376.
19. G. Sharma, H. J. Trussell and M. J. Vrhel, Optimal nonnegative color scanner filters, *IEEE Trans. Image Proc.*, **7**(1), 129-133 (1998).
20. R. Luther, Aus Dem Gebiet der Farbreizmetrik, *Z. Technol. Phys.* **8**, 540-558 (1927).
21. S. Quan and N. Ohta, Evaluating quality factors of hypothetical spectral sensitivities, *Proc. IS&T PICS 2000*, IS&T, Springfield, VA, 2000, pp. 37-42.
22. G. H. Golub, C. F. Van Loan, *Matrix Computations*, Johns Hopkins Univ. Press, Baltimore, MD (1989).
23. P. D. Burns and R. S. Berns, Error propagation Analysis in color measurement and imaging, *Color Res. Appl.* **22**(4), 280-289 (1997).
24. G. C. Holst, *CCD Arrays, Cameras and Displays*, SPIE Optical Engineering Press, Bellingham, WA, 1999.
25. P. D. Burns, *Analysis of Image Noise in Multispectral Color Acquisition*, Ph.D. Dissertation, Rochester Institute of Technology, Rochester, NY, USA (1997).
26. J. R. Magnus and H. Neudecker, *Matrix Differential Calculus with Applications in Statistics and Econometrics*, John Wiley & Sons, Chichester, UK (1999).
27. G. Sharma, Color Scanner Characterization, Performance Evaluation, and Design, Ph.D. Dissertation, North Carolina State University, Raleigh, NC, USA (1996).
28. G. Wyszecki and W. S. Stiles, *Color Science*, John Wiley and Sons, Inc. New York (1982).